Environmental Pollution 160 (2012) 109–117

Contents lists available at SciVerse ScienceDirect

Environmental Pollution

journal homepage: www.elsevier.com/locate/envpol

Insights into low fish mercury bioaccumulation in a mercury-contaminated reservoir, Guizhou, China

Bian Liu[a,1], Haiyu Yan[b], Cuiping Wang[b], Qiuhua Li[b,c], Stéphane Guédron[a,2], Jorge E. Spangenberg[d], Xinbin Feng[b,*], Janusz Dominik[a]

[a] Institute F. -A. Forel, University of Geneva, route de Suisse 10, C.P. 416, CH-1290 Versoix, Switzerland
[b] State Key Laboratory of Environmental Geochemistry, Institute of Geochemistry, Chinese Academy of Sciences, 46 Guanshui Road, Guiyang 550002, China
[c] Key Laboratory for Information System of Mountainous Area and Protection of Ecological Environment of Guizhou Province, Guizhou Normal University, Guiyang 550002, China
[d] Institute of Mineralogy and Geochemistry, University of Lausanne, CH-1015 Lausanne, Switzerland

ARTICLE INFO

Article history:
Received 28 March 2011
Received in revised form
2 September 2011
Accepted 14 September 2011

Keywords:
Mercury
Monomethylmercury
Bioaccumulation
Reservoir
Fish

ABSTRACT

We examined Hg biogeochemistry in Baihua Reservoir, a system affected by industrial wastewater containing mercury (Hg). As expected, we found high levels of total Hg (THg, 664–7421 ng g^{-1}) and monomethylmercury (MMHg, 3–21 ng g^{-1}) in the surface sediments (0–10 cm). In the water column, both THg and MMHg showed strong vertical variations with higher concentrations in the anoxic layer (>4m) than in the oxic layer (0–4 m), which was most pronounced for the dissolved MMHg ($p < 0.001$). However, mercury levels in biota samples (mostly cyprinid fish) were one order of magnitude lower than common regulatory values (i.e. 0.3–0.5 mg kg^{-1}) for human consumption. We identified three main reasons to explain the low fish Hg bioaccumulation: disconnection of the aquatic food web from the high MMHg zone, simple food web structures, and biodilution effect at the base of the food chain in this eutrophic reservoir.

1. Introduction

Mercury (Hg) is a globally distributed toxic pollutant. Monomethylmercury (MMHg) is one of the toxic Hg forms that can bioaccumulate and biomagnify in food webs (Clarkson and Magos, 2006; Fitzgerald et al., 2007; Ullrich et al., 2001; Watras et al., 1998). Humans and wildlife that are high in the food chain are subject to potential adverse health effects related to MMHg exposure via the consumption of fish and fish products (Clarkson and Magos, 2006). The public health concern of MMHg have prompted numerous studies on Hg biogeochemical cycling in aquatic systems.

Reservoirs are important aquatic systems to communities that depend on them for resources such as drinking water, fisheries, and irrigation. The exact mechanisms of Hg cycling and the bioaccumulation of MMHg in reservoirs have not been well understood. As in other systems, the rise and fall of Hg levels in reservoirs are results of many interrelated factors (Benoit et al., 2003; Compeau and Bartha, 1985; Munthe et al., 2007) including Hg loading rates, water chemistry (e.g. dissolved organic matter; sulfate concentrations; redox potential, and pH, etc.), microbial activities, and food web structures.

Starting from 2009, we have been studying the distribution of mercury in different matrices and understanding the mechanism of mercury methylation and the consequent bioaccumulation in Baihua Reservoir (BR) in China as part of a 3-year Sino-Swiss project. The ecosystem of BR has become increasingly vulnerable due to various environmental problems (e.g. eutrophication, algal blooms) including direct Hg contamination from Guizhou Organic Chemical Plant (GOCP). The GOCP is located ~18 km upstream of BR and used mercury as a catalyst for the production of acetic acid (Feng et al., 2004) with an estimated 573 tons of Hg being used between 1971 and 1985 (Yan et al., 2008). Wastewater containing Hg was directly discharged before the installation of Hg-removal treatment facility in 1985 (Yan et al., 2008). Later, mercury-based-technique was gradually replaced by the methanol carbonylation technique but variable, sometimes high, total Hg (THg) concentrations were detected in the wastewater canals (Zhang, 2000). Elevated THg concentrations were also reported in the wastewater outfall of GOCP ([THg] = 13 ng L^{-1}; Horvat et al., 2003). Due to the high Hg levels, there is a growing need to study Hg dynamics in BR

* Corresponding author.
E-mail addresses: bl2444@columbia.edu (B. Liu), guedrons@ujf-grenoble.fr (S. Guédron), fengxinbin@vip.skleg.cn (X. Feng).
[1] Present address: Department of Medicine, Columbia University, New York, NY 10032, USA.
[2] Present address: Institut des Sciences de la Terre (ISTerre), UMR 5559 (IRD/UJF/CNRS), Université Joseph Fourier, BP 53, F-38041, Grenoble, France.

0269-7491/$ – see front matter © 2011 Elsevier Ltd. All rights reserved.
doi:10.1016/j.envpol.2011.09.023

and to investigate whether consumption of BR fish poses potential human health risks.

Previous studies conducted in BR showed that while elevated THg and MMHg levels were found in the water column (average [THg] = 35.9 ng L^{-1}, Yan et al., 2003) and sediment porewater ([THg] = 6–5860 ng L^{-1}, [MMHg] = 0.3–15.4 ng L^{-1}; Yan et al., 2008), THg concentrations in fish muscles (Cyprinidae, commonly known as carp) were generally low with variations between species (0.3–39 ng g^{-1}; Horvat et al., 2003; Yan et al., 2003, 2008). These findings are in contrast to the high fish Hg burden reported for more pristine lakes and reservoirs in North America and northern Europe (Larssen, 2010; Munthe et al., 2007). While fish Hg concentrations are often positively correlated with the THg input to the system, the relationships between the two are far from simple. The counterintuitive observations of the low fish Hg concentrations in BR requires a more detailed analysis of factors related to the source, transformation, and the bioaccumulation of MMHg. In this paper, by relating Hg concentrations in biota samples with those in abiotic matrices, we aim to provide some insights into the factors influencing fish Hg bioaccumulation in BR.

2. Materials and methods

2.1. Study sites

Baihua Reservoir (106°27′–106°34′ N, 26°35′–26°42′ E) is located approximately 16 km northwest of Guiyang, Guizhou Province, southwest China. Since its impoundment in 1966, BR has been providing the local communities with hydropower, fisheries, irrigation, drinking water, and recreation resources. It is a long and narrow reservoir (L × W = 18 km × 0.8 km) with an average water depth of 13 m (Yan et al., 2008) and an average water residence time of one month (Li et al., 2008; Wang et al., 2005). Baihua Reservoir is one of the reservoirs built on the Maotiao River and its closest neighbor is Hongfeng Reservoir (~20 km upstream). Besides Maotiao River, there are a few seasonal streams/rivers with limited contributions to the total water input of BR. The ratio of the total surface area of BR (14.5 km^2) to the whole watershed area is 0.77%. The reservoir has a typical karstic topography with limestone and dolomite being the dominant bedrock types and calcareous soil and ultisol being the major soil types. Because of steep slopes that are typically present in such topography, the shallow littoral zone has small surfaces and is generally limited to areas at the stream mouths, despite having no shortage of islands.

To investigate the biogeochemical cycling of Hg in the water column and the sediment, we chose three study sites (Y, M, and D) representing the upper, middle, and lower reaches of the pelagic part of the reservoir, respectively. The water depths at these three sites were 12, 20, and 21 m, respectively. Due to the persistent oxycline (anoxic below 4 m in this study in 2009), we did not find benthic fauna (i.e. chironomid larvae) in the sediment under the pelagic zone. Alternatively, we selected two shallow sites (i.e. YS and DS) with an average water depth of ~0.5 m in the littoral zone to investigate the bioaccumulation of Hg in benthic invertebrates.

2.2. Sample collection (main sampling in June, 2009)

2.2.1. Water column samples

Water samples were made using a 10-L Niskin bottle and filtered (0.45 μm, Sterivex®-HV, Millipore) for the dissolved Hg species (i.e. THg_{dis} and $MMHg_{dis}$) and those associated with suspended solids (i.e. THg_{ss} and $MMHg_{ss}$). Whatman (GF/F) glass-fiber filters were used for the dissolved organic carbon (DOC) samples. Ancillary variables such as total phosphate (TP), total nitrogen (TN), and Chlorophyll a (Chl-a) were also measured according to methods described by Li and Han (2007). Water column parameters such as dissolved oxygen (DO), temperature, and conductivity

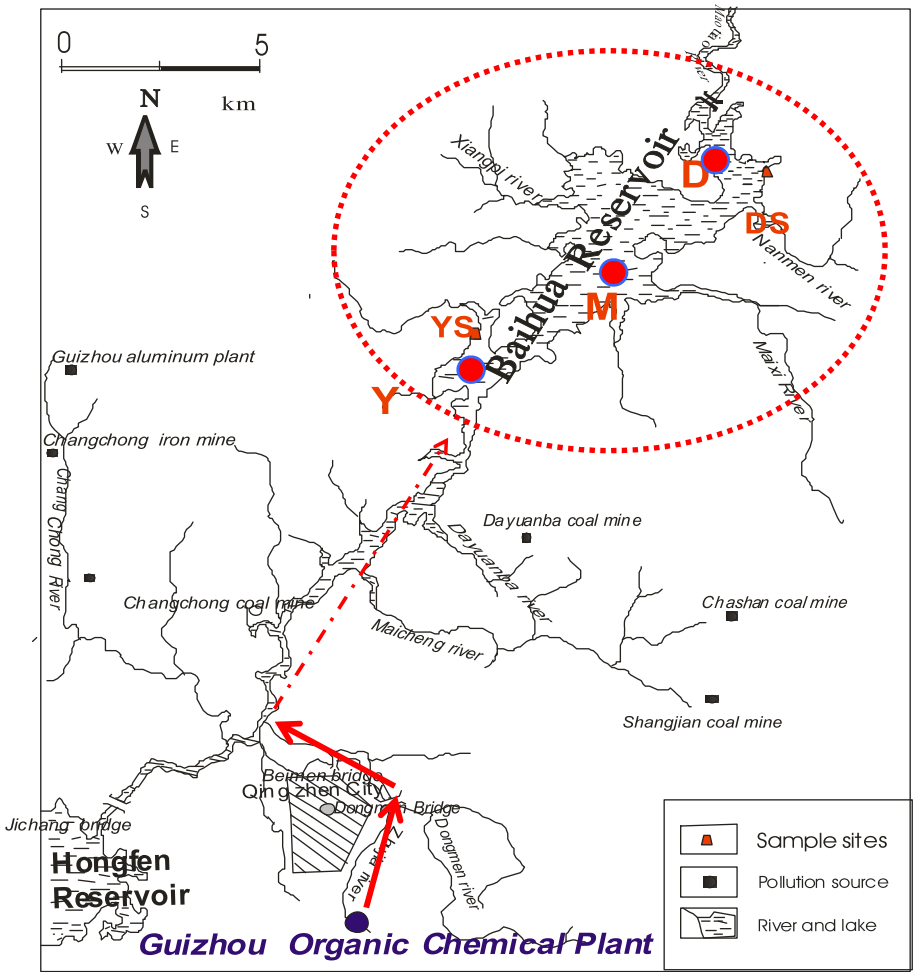

Fig. 1. Locations of the study sites, which include three main study sites Y, M, and D that are located in the upper, middle, and lower reaches of the reservoir, respectively; and two littoral zone sites (YS and DS). Arrows highlight the pathway of mercury contamination from the known point source (i.e. Guizhou Organic Chemical Plant).

were measured in situ using a multi-parameter probe (Radiometer, Pioneer 65) while water hardness (in mg $CaCO_3$ L^{-1}) was measured using a Winkler kit.

2.2.2. Sediment samples

Surface sediments (0–10 cm) were taken using a gravity corer. Within a few hours of collection, sediment cores were sectioned with a 2-cm increment in a N_2-atmosphere-glovebag in a laboratory by the reservoir. After centrifugation, porewater was filtered (0.45 μm) and the pulled supernatant was divided for the analysis of porewater THg (THg_{pw}), MMHg ($MMHg_{pw}$), and ancillary variables.

2.2.3. Biota samples

Seston used for Hg analysis were collected in the surface water (~0.5 m) using towing nets with 64 and 112 μm mesh sizes, respectively (Li and Han, 2007). Chironomid insect larvae (not identified to the genus level) were collected by sieving (900 μm) the surface sediments (~0–4 cm) from YS and DS sites (Fig. 1), followed by rinsing in deionized water, EDTA (1 mM), and deionized water, for 5 min each. After drying with clean paper towels, the larvae were quickly frozen in liquid nitrogen on site.

Fish were collected from the local anglers. The dominant species available from BH were species of the fish family Cyprinidae (commonly called carp), which is also the typical fish species consumed locally. After recording the length and mass, fish axial muscles were collected under clean conditions, and subsequently frozen until analysis. In order to better assess the biota Hg levels in BR, we also used data from June 2010 sampling and from earlier studies (i.e. in autumn and winter of 2003 and 2008; Yan, 2005; Yan et al., 2008, 2010). Axial fish scales from 2009 and a subset of 2003 samples were also collected for the identification of fish age.

2.3. Sample analysis

Total Hg and MMHg in the sediment, chironomid larvae, seston, 2010 fish samples of 5 species ($n = 13$), and $MMHg_{ss}$ were analyzed in the Swiss laboratory. THg was analyzed using thermal combustion method (AMA 254, Leco®). MMHg in solid matrix was extracted using a HNO_3 leaching/CH_2Cl_2 extraction method, followed by ethylation onto Tenax® traps, GC separation (Bloom, 1989), and atomic florescence spectrometry (AFS) detection by Tekran® (Model 2500, Tekran Inc., Canada). Briefly, the extraction involves the following steps: (1) weigh ~0.3 g of freeze-dried homonogized samples into a 50 mL centrifuge tube; (2) add 2 ml $CuSO_4$ (1M), 5 ml HNO_3 (5M), and 10 mL CH_2Cl_2; (3) shake the mixture for 1 h; (4) centrifuge the mixture for 25 min at 3000 rpm; (5) pipette the solvent layer into a new 50 mL centrifuge tube; (6) back extract MMHg into 35 mL deionized water under N_2 flow (50 mL min^{-1}) for 30 min in a water bath (50 °C). THg_{ss} was analyzed using HCl/HNO_3 digestion followed by AFS detection (Cossa et al., 2002). Aqueous samples, fish samples from 2009 and earlier years were analyzed in the Chinese laboratory and the methods were described elsewhere (Yan, 2005; Yan et al., 2008, 2010). Analytical methods for TP, TN, and Chl-a were described previously (Li and Han, 2007) and DOC was analyzed by high-temperature catalytic oxidation method (Li et al., 2008). Carbon and nitrogen isotope analysis was conducted for the 2010 biota samples at the Stable Isotopes Laboratory of the University of Lausanne (UNIL), Switzerland. Results were expressed as $\delta^{13}C$ and $\delta^{15}N$ values as the per mil (‰) deviations of the isotope ratio relative to known standards (C: Vienna Pee Dee Belemnite; N: atmospheric nitrogen) using the following formula: $\delta X = [(R_{sample} - R_{standard})/R_{standard}] \times 1000$, where R is the ratio of the heavy to light isotopes (and X is $^{13}C/^{12}C$ or $^{15}N/^{14}N$).

2.4. QA/QC and data analysis

Samples for dissolved phase Hg species were acidified (HCl, 0.5%, v/v), stored in acid cleaned borosilicate glass tubes, while samples for redox sensitive parameters (e.g. Fe^{2+}, and S^{2-}) were stored in 10 mL serum vials and crimp sealed. Aqueous samples were kept in the dark at 4 °C and analyzed within three weeks of collection while solid phase samples were kept frozen until analysis. The average (arithmetic mean ± 1 standard deviation (SD)) relative standard deviations (RSDs) of replicates were 9 ± 5% ($n = 24$ pairs), 17 ± 5% ($n = 37$ pairs), 4 ± 2% ($n = 2$ pairs), and 11 ± 10% ($n = 28$ pairs) for THg, MMHg, DOC, and ions, respectively. Three certified reference materials (i.e. BEST-1, MESS-3, and Tort-2) were used in the analysis of THg in solid matrices while two (i.e. ERM-CC580 and Tort-2) were used for MMHg. The average recoveries were 98 ± 7% ($n = 11$) and 106 ± 11% ($n = 29$) for THg and MMHg, respectively. The calibration, reproducibility, and accuracy of the C and N isotopic analysis were based on laboratory standard materials replicates (C: glycine, urea, Pyridine, USGS-24, UNIL-graphite; N: glycine, urea, pyridine, UNIL-graphite, USGS-40, USGS-41, USGS-24 graphite, IAEA-600, and IAEA-N3) and were better than 0.1‰ (1 SD) for both isotopes. The RSDs of replicates of samples ($n = 22$ pairs) were better than 2%.

Statistical analyses were conducted using SPSS (v.15). Nonparametric methods (e.g. Kruskal–Wallis test) and natural log transformation of the data (for linear regression analysis) were performed. In the box plots presented, the line inside the box shows the median; the length of the box is the interquartile range (IQR = 75th percentile–25th percentile); the left/bottom and right/top whiskers show the distance from the end of the box to the smallest and largest values that are 1.5 IQR from either end of the box, respectively; "o" indicates outliers, defined as values between 1.5 IQR and 3 IQR's from the end of the box; and "*" indicates extreme values, defined as values more than 3 IQR's from the end of the box. Unless otherwise stated, mercury concentrations were expressed in ng L^{-1} for the dissolved phase in the porewater and water column; in ng g^{-1} dry wet (dw) for the solid sediment, suspended solids, seston, and chironomid larvae; and in ng g^{-1} wet weight (ww) for fish. The water column total Hg and total MMHg were calculated as the sum of the dissolved and the suspended solid-bound fraction, the latter of which was converted into ng L^{-1} unit based on the volume of water filtered.

Bioaccumulation factor (BAF, Gobas et al., 2009) was calculated as the ratio of MMHg concentrations in biota samples (ng g^{-1} ww) to the dissolved water concentration (ng L^{-1}) in the oxic layer of the water column. The water content used

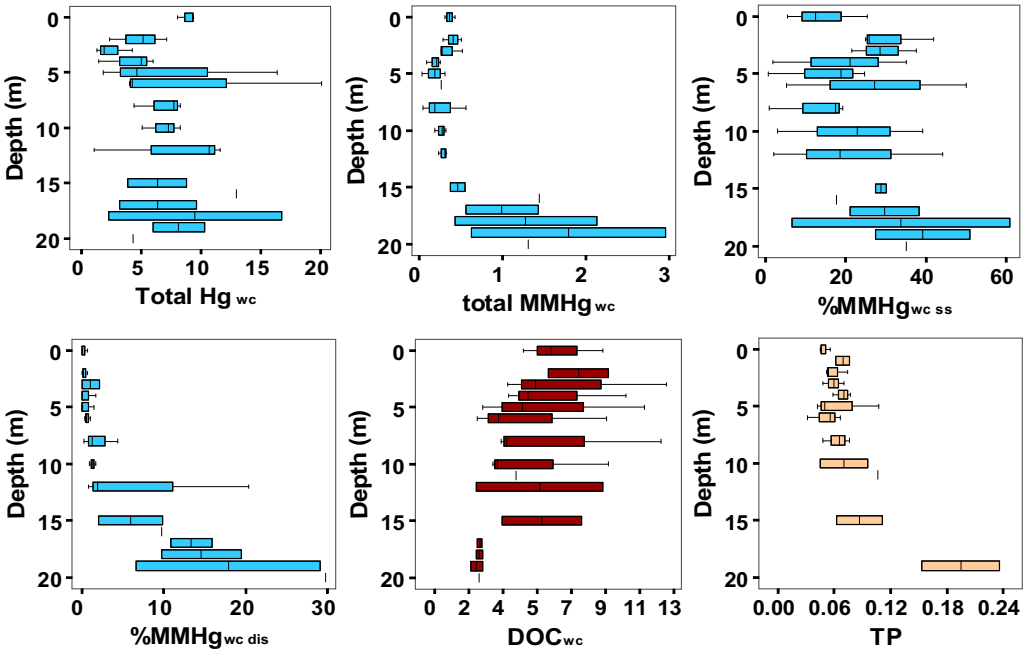

Fig. 2. Box plots of water column depth profiles of total Hg and total MMHg (i.e. THg_{wc} and $MMHg_{wc}$ in ng L^{-1}, total = dissolved + suspended solid-bound), %MMHg in the dissolved (%$MMHg_{wc, dis}$) and suspended solids (%$MeHg_{wc, ss}$), DOC (mg L^{-1}), and TP (mg L^{-1}) in Baihua Reservoir sampled in June 2009. Data shown are reservoir-wide values, i.e. combined results from Y, M, and D sites.

Table 1
Concentrations (average ±1 standard deviation (median)) of THg and MMHg in abiotic matrices and biota samples of Baihua Reservoir.

	Sample type	THg	MMHg	%MMHg	N
Biota	Fish[a]	48.7 ± 45.3 (34.5)	16 ± 9.4 (14.6)	46.5 ± 21.8 (46)	128
	Chironomid larvae[b]	205.6 ± 71.6 (242.1)	9.4 ± 11.1 (4.7)	6.7 ± 4.0 (5.2)	3
	Seston < 64 μm[c]	862.4 ± 507.8 (750)	4.0 ± 2.7 (4.3)	0.6 ± 0.6 (0.6)	4
	Seston < 112 μm[c]	724.4 ± 410.4 (727)	2.7 ± 0.4 (2.8)	0.5 ± 0.3 (0.4)	4
Sediment	Solid sediment	3677 ± 2596 (3413)	8.8 ± 4.9 (6.6)	0.4 ± 0.3 (0.4)	15
	Porewater	n.a.	0.8 ± 1.2 (0.3)	n.a.	15
Water column	Dissolved phase				
	Oxic	3.3 ± 2.2 (3.4)	0.02 ± 0.02 (0.01)	0.5 ± 0.8 (0.07)	12
	Anoxic	5.7 ± 3.9 (4.6)	0.4 ± 0.6 (0.1)	7.2 ± 9.1 (1.9)	25
	Whole	4.9 ± 3.6 (3.7)	0.3 ± 0.5 (0.05)	5.2 ± 8.1 (1.3)	37
	Suspended solids				
	Oxic	185.2 ± 97.8 (155.2)	9.8 ± 6.9 (7.8)	7.7 ± 7.9 (5.8)	12
	Anoxic	441.8 ± 499.5 (259.8)	19.9 ± 19.2 (17.7)	8.1 ± 9.4 (5.6)	25
	Whole	358.5 ± 429.1 (241.8)	16.6 ± 16.8 (10.5)	8.0 ± 8.8 (5.8)	37
	Total				
	Oxic	5.1 ± 3.0 (5.1)	0.3 ± 0.1 (0.3)	10.1 ± 10.1 (5.9)	12
	Anoxic	7.7 ± 4.9 (7.3)	0.6 ± 0.7 (0.3)	10.1 ± 9.1 (6.8)	25
	Whole	6.9 ± 4.5 (6.0)	0.5 ± 0.6 (0.3)	10.3 ± 9.5 (6.7)	37

Note: Arithmetic means are reported. Abiotic matrices (i.e. sediment and water column) were sampled in June. 2009. n.a. = not available. Units for [Hg] in "solid sediment", "suspended solids (ss)", and biota are in ng g^{-1} dry weight (dw) while [fish Hg] is in ng g^{-1} wet weight (ww); [Hg] in "porewater", "dissolved phase", and "whole" in the water column are in ng L^{-1}.

[a] [Hg] were based on axial muscles. Data included those from this study (sampled in June 2009 and June 2010) and from previous studies (Yan, 2005; Yan et al., 2008, 2010). %MMHg were based on 23 samples where both MMHg and THg data were available. Species specific [Hg] are presented in Table 3 and Fig. 4.

[b] Chironomid larvae were collected in June 2009, January and June 2010.

[c] Seston samples were collected in June 2009 and June 2010.

in converting ng g^{-1} dw to ng g^{-1} ww for sestion (<64 μm and <112 μm) and chironomid larvae was assumed to be 90%, 85%, and 75%, respectively (USEPA, 2010).

Considering the dynamic nature of the biotic matrices (e.g. the habitat of fish is the entire reservoir and is not restricted to the three main sites where abiotic samples were taken), we grouped mercury and ancillary variables from the three main study sites to provide a reservoir-wide distribution. Nonetheless, site-specific are also provided.

3. Results and discussion

3.1. Hg in the water column

In the water column, the oxycline (DO < 0.3 mg L^{-1}) and thermocline (i.e. temperature changed from 23 °C to 17 °C) were found at ~4 m. Higher DOC was found in the epilimnion than in the hypolimnion (medians, 6.0 vs. 3.3 mg L^{-1}) which was opposite to the TP depth profile (Fig. 2). Baihua reservoir is eutrophic with the average levels of TP, TN, and Chl-a being 0.07 ± 0.04 mg L^{-1}, 1.7 ± 0.5 mg L^{-1}, and 54.7 ± 53.3 μg L^{-1}, respectively. The Secchi disk transparency was approximately 1 m, and the average pH and water hardness was 8 and 286 ± 43 mg L^{-1}, respectively.

Elevated concentrations of total Hg (i.e. $THg_{dis} + THg_{ss}$) and total MMHg (i.e. $MeHg_{dis} + MeHg_{ss}$) were found in the water column of BR with levels ranging from 1.0 to 20.1 ng L^{-1} and from 0.03 to 2.96 ng L^{-1}, respectively (Table 1, Fig. 2). In comparison, THg and MMHg values in uncontaminated freshwater systems are generally less than 5 ng L^{-1} and between 0.02 and 0.1 ng L^{-1}, respectively (Ullrich et al., 2001). The average levels of water column THg and THg_{dis} in BR (6.9 ± 4.5 and 4.9 ± 3.4 ng L^{-1}, respectively) were similar to those in Hongfeng Reservoir (6.9 and 4.0 ng L^{-1}, respectively, He et al., 2008), which is upstream of both BR and GOCP with no known Hg point sources. However, the maxima of THg and THg_{dis}, in BR were 1.4X and 2X higher, respectively. In BR, while a majority of THg was in the dissolved form (medians, 61% and 80% in the oxic and anoxic layer, respectively), a majority of the MMHg were associated with suspended solids with $MMHg_{ss}$ representing 61% and near 100% of MMHg in the anoxic and oxic waters, respectively (Table 1).

Both THg and MMHg showed strong vertical gradients, with higher values found in the anoxic layer (>4 m) than in the oxic layer (Table 1). Similarly, the percentage of MMHg present in THg (i.e. % MMHg = [MMHg]/[THg] × 100) also showed higher levels in the anoxic layer (Table 1, Fig. 2). However, the difference between the oxic and anoxic zones wase only statistically significant (Mann–Whitney tests, $p < 0.001$) for $MMHg_{dis}$ and $\%MMHg_{dis}$. The trend of higher anoxic $MMHg_{dis}$ than its oxic counterpart was also seen in 2004 (unpublished data). Similar depth profile was reported for eutrophic and seasonally stratified Onondaga Lake, where $MMHg_{dis}$ ranged from 0.06 to 0.1 ng L^{-1} in the mixed water column in spring and up to 5.4 ng L^{-1} in the bottom anoxic water in the summer (Todorova et al., 2009).

The levels of all measured Hg species in the oxic layer were not significantly different among the three sampling sites (Kruskal–Wallis test, $p > 0.05$), except for $MMHg_{ss}$ ($p = 0.02$). Site M had the highest $MMHg_{ss}$ concentration (medians, 12.7, 7.3, and 6.9 ng L^{-1}, for M, Y and D, respectively), which was perhaps due to its proximity to a small river mouth and the pier of the reservoir (more water traffic), thus more physical disturbance and suspension in the water column than Sites Y and D. It is worth noting that the oxycline at 4 m in BR did not coincide with the sharp gradient of MMHg concentrations (Fig. 2), which occurred below 4 m with the most pronounced gradients appeared around 15 m at M and D. Interestingly, the bottom water column MMHg levels at Sites M and D were 82% and 48% higher than their sediment porewater counterparts (0–2 cm), respectively. The observed depth porfiles of $MMHg_{ss}$ may be related to several factors such as non-linear diffusion rates at different depths, and the dominance of methylation or demethylation at different depths. We found that $MMHg_{dis}$ was positively correlated with TP ($R^2 = 0.25$, $n = 22$, $p < 0.05$) but negatively correlated with DOC ($R^2 = 0.18$, $n = 29$, $p < 0.05$). The similarity in the depth profiles of TP and $MMHg_{dis}$ (Fig. 2) suggests a higher release of MMHg related to the degradation of settling organic matter deeper than 15 m, while the anticorrelation between DOC and $MMHg_{dis}$ suggests a higher removal of MMHg by particles shallower than 15 m. The high $MMHg_{dis}$ could also result from methylation in the bottom anoxic water, though our water column experiment using enriched Hg isotopes conducted at M site in 2010 showed substantially higher demethylation than methylation potential rates (data not shown). The exact mechanism producing the observed $MMHg_{dis}$ profiles remains unclear at this

Table 2
Comparisons of mercury concentrations in Cyprinidae (ng g^{-1} ww) and water column dissolved phase (ng L^{-1}) and/or in sediments (ng g^{-1} dw) from selected studies (min-max and/or average ±1 standard deviation).

Sediment Hg (ng g^{-1} dw)		Water Column Hg (ng L^{-1})		Fish Hg (ng g^{-1} ww)			Weight (carp species) (g)	Length (cm)	Study sites	References
THg	MMHg	THg	MMHg	THg	MMHg	%MMHg				
		1–8 (6.9)		8–103			80–7735 (bc, cmc, gc)	11–82	Hongfeng Reservoir, China; upstream of BR	He et al., 2008; Yan et al., 2010
				28–129			(bc, sc)	54–88	Illinois & Mississippi Rivers, US	Rogowski et al., 2009
57–1670				3–44*			(bc, cmc, gc, sc)	25–48	Hong Kong, Pearl River Delta, China	Zhou and Wong, 2000
				50–300			(cmc)	25–55	Lake Meredith, Texas, US	McClain et al., 2006
				19–63	18–63	75–110	1790–3290 (cmc, 4 y)	40–48	Ponds in Czech. No obvious point sources	Marsalek et al., 2007
70–170,000				70–1090			(cmc)	49–69	Ebro River, Spain. Contaminated by chloralkali plant.	Navarro et al., 2009
700–3300	7–28	3–9	0.2–5	4600–5500			56–132 (crc; 1–2 y)	15–21	Babeni Reservoir, Romania. Contaminated by chloralkali plant	Bravo, 2011
665–7421	3–21	1–20 (6.9 ± 4.5)	0.03–3 (0.5 ± 0.6)	4–254 (53 ± 49)	3–39 (16 ± 9)	16–79 (46 ± 18)	70–4860 (862 ± 856) (bc, cmc, crc,gc, sc; 1–4 y)	12–62 (33 ± 12)	Baihua Reservoir, China. Contaminated by organic chemical plant.	This study

Note: bc = big-head carp = *Hypophthalmichthys nobilis*; cmc = common carp = *Cyprinus carpio*; crc = crucian carp = *Carassius carassius*; gc = grass carp = *Ctenopharyngodon idella*; sc = silver carp = *Hypophthalmichthys molitrix*. y = fish age in year. *, [Hg] in wet weight (ww) was calculated from dry weight (dw) assuming 80% water content.

time. Further studies are needed to elucidate the water column Hg dynamic in details.

3.2. Hg in the sediments

As expected for a point-source contaminated site, THg_{sed} (3677 ± 2596 ng g^{-1}) and $MMHg_{sed}$ (8.8 ± 4.9 ng g^{-1}) at BR were both elevated (Table 1). The THg levels in BR were similar to values (Table 2) reported for sites contaminated by chloralkali industries such as the Babeni Reservoir (Bravo, 2011) and Ebro River (Navarro et al., 2009). Compared to the levels in Hongfeng Reservoir (He et al., 2008), the concentrations of THg_{sed} and $MMHg_{sed}$ in BR were approximately 10 and 4 folds higher, respectively.

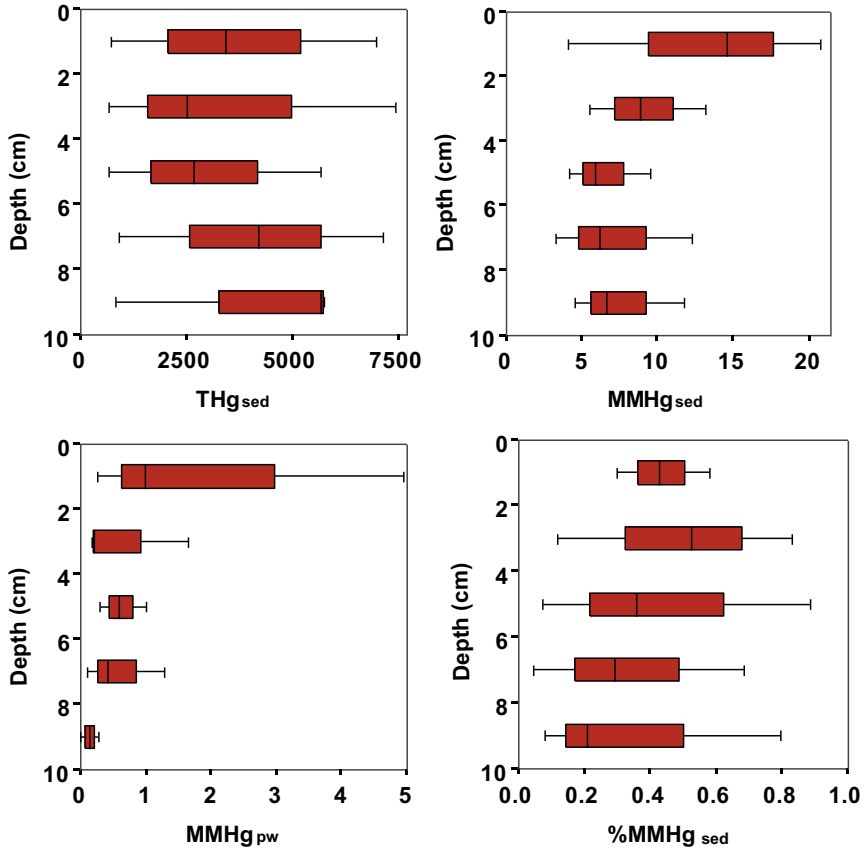

Fig. 3. Box plots of sediment depth profiles of THg, MMHg, %MMHg in the solid sediment (THg_{sed}, $MMHg_{sed}$ in ng g^{-1} dw, and $\%MMHg_{sed}$), and MMHg in sediment porewater ($MMHg_{pw}$ in ng L^{-1}) in Baihua Reservoir sampled in June 2009. Data shown are reservoir-wide values, i.e. combined results from Y, M, and D sites.

The spatial pattern of mercury also indicated a typical contaminated system, where THg concentrations in the solid sediment and MMHg in porewater tend to decrease with increasing distance from the GOCP (i.e. Y > M > D). Mainly driven by the spatial distribution of THg, $\%MMHg_{sed}$ showed a sharp increase along the direction of the water flow (i.e. Y < M < D). The maximum $MMHg_{pw}$ found at Y was consistent with the distribution of porewater DOC (DOC_{pw}), where Y site had the highest level (medians, 11.4, 10.0, and 7.0 mg L^{-1} for Y, D and M, respectively). However, we did not find statistically significant correlations between porewater DOC and MMHg.

The depth profiles of the sediment mercury concentrations suggest in situ methylation at the water–sediment interface of BR. Both $MMHg_{pw}$ and $\%MMHg_{pw}$ in the sediment tend to peak at the surface sediment (0–4 cm, Fig. 3) similar to the trend found in $MMHg_{sed}$, and also similar to the depth profiles of redox sensitive elements such as S^{2-} and Fe^{2+} (data not shown). The overall porewater S^{2-} was less than 10 μM, which was within the predicted optimal sulfide levels that favor the uptake of neutrally charged Hg species via passive diffusion by methylators (Benoit et al., 2003). The most active zone of methylation often occurs at the water–sediment interface where methylating bacteria are most active, coinciding with the abundance of nutrient and labile organic matter as well as the redox transition zone (Fitzgerald et al., 2007; Merritt and Amirbahman, 2009). Consequently, maxima of MMHg and %MMHg are often found at the sediment–water interface as seen in BR (Fig. 3).

3.3. Hg in biota samples

Fish Hg concentrations were not correlated with any of the fish characteristics (e.g. length, mass, and age). Low THg concentrations (4–254 ng g^{-1}, $n = 128$) were found in the fish of BR (Table 3), which were one order of magnitude lower than the guideline THg values (e.g. 300–500 ng g^{-1} ww) for edible portion of fish and shellfish accepted in several regulatory guidelines for human consumption (Clarkson and Magos, 2006), similar to the result from previous studies (Horvat et al., 2003; Yan et al., 2008, 2010). The carp THg concentrations in BR (Fig. 4) were comparable to the same carp species from a variety of aquatic systems as listed in Table 2, except for those found in Babeni Reservoir, which had higher water column $MMHg_{dis}$ levels (i.e. 2–6X higher than those in the anoxic layer of BR).

When fish species were divided into four groups based on their feeding behaviors, the lowest and the highest THg concentrations were found in the herbivorous and omnivorous group, respectively (Fig. 5). Herbivorous also had larger body masses and longer body lengths than the omnivorous. No significant differences (Mann–Whitney test, $p > 0.05$) were found between the Hg concentration data from this study (i.e. sampled in 2009 and 2010)

Table 3
Species specific Hg concentrations and fish characteristics of Baihua Reservoir.

			THg	MMHg	%MMHg	Length (cm)	Weight (g)	Age (year)	$\delta^{15}N$ (‰)	$\delta^{13}C$ (‰)
Species name	*Cyprinus carpio*	Mean ± SD	50.8 ± 61.7	17.4 ± 8.8	51.7 ± 15.9	37.7 ± 12	1305.1 ± 1184.7	2.7 ± 1.1	16.2 ± 0.2	−24.8 ± 2.3
Common name	Common carp	Median	28.2	14.6	47.2	39.3	875	2.5	16.1	−24.7
Feeding type	Omnivore	Min ~ Max	4 ~ 254	9.8 ~ 30.5	30.5 ~ 69.1	12 ~ 62	70 ~ 4860	1 ~ 4	16 ~ 16.4	−27 ~ −22.6
		N	28	5	5	28	28	9	3	3
Species name	*Hypophthalmichthys nobilis*	Mean ± SD	48.5 ± 32.5	25.9 ± 9.8	48 ± 15.1	40.2 ± 9.1	1204.8 ± 703.9	2.7 ± 0.6	20.4 ± 0.2	−23.9 ± 0.2
Common name	Big-head carp	Median	40.2	24.3	52.5	39	1000.0	3	20.5	−24
Feeding type	Planktivore	Min ~ Max	20.1 ~ 143.2	15.7 ~ 39.3	27.4 ~ 59.8	24 ~ 60	400 ~ 2500	2 ~ 3	20.2 ~ 20.5	−24 ~ −23.6
		N	21	4	4	21	21	3	3	3
Species name	*Hypophthalmichthys molitrix*	Mean ± SD	23 ± 18.4	10.6 ± 7.8	34.7 ± 18.9	38.9 ± 7.8	876.2 ± 624.4	3.3 ± 0.6	17.6 ± 0.3	−24.9 ± 0.4
Common name	Silver carp	Median	19.5	8.4	28.5	40	650	3	1.74	−25.1
Feeding type	Planktivore	Min ~ Max	4.2 ~ 82.2	3 ~ 23.7	15.8 ~ 61.4	23.5 ~ 52.5	300 ~ 3000	3 ~ 4	17.4 ~ 18	−25.2 ~ −24.5
		N	21	6	6	21	21	3	3	3
Species name	*Carassius carassius*	Mean ± SD	83.2 ± 46.5	17.4 ± 6.4	54.4 ± 22.1	20.4 ± 2.8	228.6 ± 106.3	1.7 ± 0.8	15.9 ± 6.6	−24.3 ± 0.2
Common name	Crucian carp	Median	88.6	15.5	52.2	20.4	200	1.5	18.3	−24.3
Feeding type	Omnivore	Min ~ Max	9.6 ~ 204	12.1 ~ 26.3	34.5 ~ 78.8	16 ~ 26.5	96.6 ~ 500	1 ~ 3	8.4 ~ 21	−24.7 ~ −24.3
		N	30	4	4	30	30	8	3	3
Species name	*Ctenopharyngodon idella*	Mean ± SD	14.4 ± 1.8	6.1	46.8	32.3 ± 2.7	690 ± 176.6	3		
Common name	Grass carp	Median	13.6			31	630			
Feeding type	Herbivore	Min ~ Max	13 ~ 17.1			30 ~ 35.5	550 ~ 970			
		N	5	1	1	5	5	1		
Species name	*Hemiculter bleekeri bleekeri*	Mean ± SD	31.1 ± 12.1	7.5 ± 5.7	23.9 ± 19.1	13.5 ± 2	10	1		
Common name		Median	30.8	7.5	23.9	13	10	1		
Feeding type	Omnivore	Min ~ Max	17.3 ~ 63	3.5 ~ 11.5	10.4 ~ 37.4	10 ~ 16.5	10	1		
		N	11	2	2	11	11	2		
Species name	*Pelteobagrus fulvidraco*	Mean ± SD	41.4 ± 16			20.2 ± 2.3	236.7 ± 77.4			
common name	yellow-head catfish	Median	45.6			20.3	220.0			
Feeding type	Carnivore	Min ~ Max	13.1 ~ 61.2			17 ~ 23	150 ~ 350			
		N	6			6	6			
Species name	*Abbottina obtusirostris*	Mean ± SD	31.5 ± 19.4	23.5	100	8			19.5	−25.1
Common name		Median	20.6							
Feeding type	Carnivore	Min ~ Max	20 ~ 53.9							
		N	3	1	1	2			1	1
Species name	*Clarias fuscus*	Mean ± SD	19.4 ± 6.5			39.8 ± 16.9	700 ± 526.8			
Common name	catfish	Median	16			45	650			
Feeding type	Carnivore	Min ~ Max	15.4 ~ 27			21 ~ 53.5	200 ~ 1250			
		N	3			3	3			

Note: ww = wet weight; mean = arithmetic mean; SD = standard deviation. [Hg] were based on axial muscles. Data included those from this study (sampled in June 2009 and June 2010) and from previous studies (Yan, 2005; Yan et al., 2008, 2010). %MMHg values were based on 23 samples where both MMHg and THg data were available. Axial fish scales from 2009 and a subset of 2003 samples were used for the fish age identification. Biota samples from 2010 were used for $\delta^{13}C$ and $\delta^{15}N$ analysis.

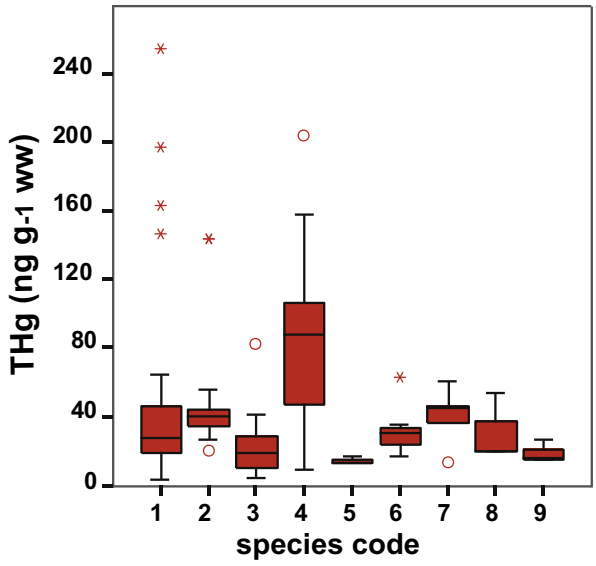

Fig. 4. Baihua Reservoir fish Hg concentrations (ng g^{-1} ww). Latin names (common names) for the species code from 1 to 9 on the *X*-axis are 1 = *Cyprinus carpio* (common carp, $n = 28$), 2 = *Hypophthalmichthys nobilis* (big-head carp, $n = 21$), 3 = *Hypophthalmichthys molitrix* (silver carp, $n = 21$), 4 = *Carassius carassius* (crucian carp, $n = 30$), 5 = *Ctenopharyngodon idella* (grass carp, $n = 5$), 6 = *Hemiculter bleekeri bleekeri* ($n = 11$), 7 = *Pelteobagrus fulvidraco* (yellow-head catfish, $n = 6$), 8 = *Abbottina obtusirostris* ($n = 3$), and 9 = *Clarias fuscus* (catfish, $n = 3$), respectively.

and data from the earlier studies (i.e. sampled in 2003 and 2008) either for the whole data set or just for the carp species. For the same carp species, we did not find statistically significant differences (Kruskal–Wallis test, $p > 0.05$) in Hg levels among the four sampling years (Fig. 6).

For chironomid larvae and seston, while their THg levels were elevated (123–200 and 793–862 ng g^{-1}, respectively), their MMHg remained low (<10 ng g^{-1}; Table 1). The range of %MMHg in the chironomid of BR (4%–11%) was similar to those found at an unpolluted site (4–5%, Watras et al., 1998) and a gold-mine-polluted site (0.03–14.7%, (Suchanek, 2008)) but was much lower than those in a chloralkali contaminated site (26%; Becker and Bigham, 1995).

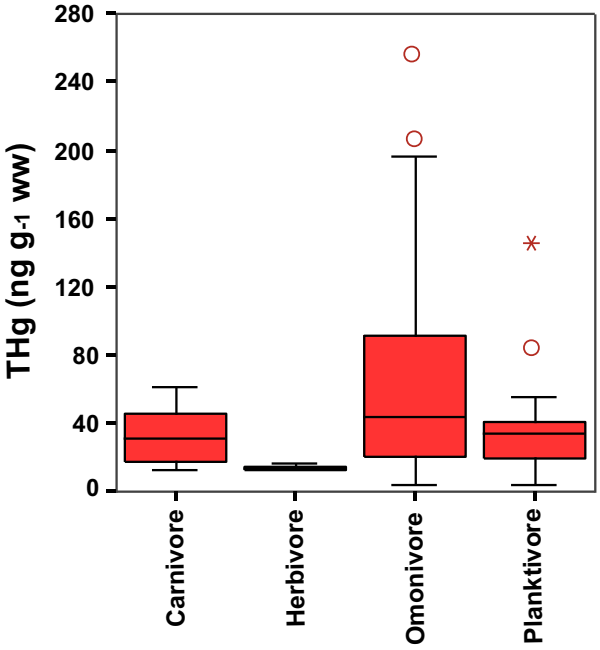

Fig. 5. Baihua Reservoir fish Hg concentrations (ng g^{-1} ww) by four feeding behavior groups. Carnivores = (*Abbottina obtusirostris, Pelteobagrus fulvidraco, Clarias fuscus.*); Herbivores = (*Ctenopharyngodon idella*); Ominivores = (*Cyprinus carpio, Carassius carassius, Hemiculter bleekeri bleekeri.*); Planktivores = (*Hypophthalmichthys nobilis, Hypophthalmichthys molitrix*).

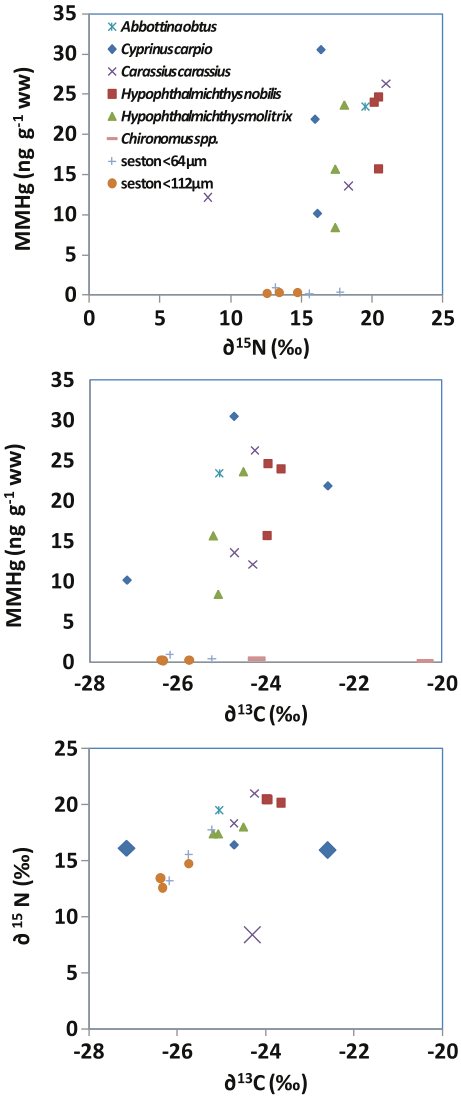

Fig. 6. Correlations between MMHg, $\delta^{13}C$, and $\delta^{15}N$. MMHg was not significantly correlated with $\delta^{13}C$ or $\delta^{15}N$. Significant $\delta^{15}N$-$\delta^{13}C$ correlation ($p < 0.01$) was only found when three possible outliers (highlighted in enlarged symbols in the bottom panel) were excluded. Individual samples from 2010 field campaign are shown, and $\delta^{15}N$ was not available for chironomid samples.

Overall, limited variations were seen in both $\delta^{13}C$ and $\delta^{15}N$ for the biota samples with ranges of −2.3‰ and 6.8‰, respectively. Seston $\delta^{15}N$ and $\delta^{13}C$ with sizes less than 64 and 112 μm were 15.5 ± 2.3‰ and-25.7 ± 0.008‰, respectively; and 13.6 ± 1.1‰ and-26.2 ± 0.004‰, respectively. Within the same fish species, variations were also generally small (<2‰ and <0.01‰ for $\delta^{13}C$ and $\delta^{15}N$, respectively. Table 3). No statistically significant correlations were found between MMHg and either of the isotopes, or between the two isotpes. However, when three possible outliers were excluded, $\delta^{13}C$ was strongly correlated with $\delta^{15}N$ (Fig. 6, $R^2 = 0.85$, $p < 0.01$, $n = 16$).

3.4. Explanations of low fish Hg

3.4.1. Disconnection of high MMHg zone and the aquatic food web

Our data showed that there was a disconnection between the high MMHg concentration zone and the habitat zone of biota in BR.

We observed that the water column was stratified and previous studies also showed that the stratification was fairly persistent and the water remained stratified between April and November (Li et al., 2008; Wang et al., 2005). This prolonged stagnant feature would have undoubtedly limited the eddy diffusion of MMHg from the hypolimnion into the epilimnion. Thus, during the major part of the year (including the growing season, i.e. warmer months), the biota in BR have limited access to high MMHg in the anoxic layer. During the short windows (i.e. December–March) when the water column is not thermally stratified, fish could be potentially exposed to the relatively high level MMHg in the deeper water. However, the water column MMHg concentration during this period is likely to be lower as methylation, which is primarily microbial mediated, is expected to be reduced due to lower temperature. Indeed, Yan (2005) found that %MMHg in the water column of BR decreased from 12% in August to 1% in March.

Since MMHg is concentrated from water by unicellular organisms (Mason et al., 1996), the uptake of $MMHg_{dis}$ by phytoplankton in the epilimnion of BR would be substantially higher if the epilimnion $MMHg_{dis}$ concentration was as high as that in the hypolimnion. However, anoxic layer $MMHg_{dis}$ in BR was statistically higher than its oxic layer counterpart. In addition, given the DOC concentration range (2–12 mg L^{-1}) and its higher epilimnion levels (medians, 6 vs. 3 mg L^{-1} in the hypolimnion; Fig. 2), the assimilation of MMHg by phytoplankton was likely to be inhibited by the presence of DOC (Lawrence and Mason, 2001). Consequently, the uptake of MMHg in fish, whose diet constitute the primary source of MMHg (Hall et al., 1997), would also be limited due to the low plankton MMHg at the base of the food chain.

3.4.2. Limited MMHg transfer in a simple food web

The simple food web structure in BR also contributes to the low MMHg found in the biota samples. The food web structure in BR is relatively simple perhaps due to the deteriorating water quality related to eutrophication and past aquaculture activities. The limited variations in both $\delta^{13}C$ and $\delta^{15}N$ (−2.3‰ and 6.8‰, respectively) indicate approximately two trophic positions. Because MMHg bioaccumulates along the food chain (Clarkson and Magos, 2006; Fitzgerald et al., 2007; Ullrich et al., 2001; Watras et al., 1998), the short food chains in BR indicate that the fish in BR would tend to bioaccumulate less Hg than predatory fish species (i.e. higher trophic positions and longer food chains) often found in Northern America and northern Europe lakes (Larssen, 2010; Munthe et al., 2007).

When comparisons were done within the carp species from BR, we found statistically significant (Kruskal–Wallis test, $p = 0.001$, $n = 105$) differences in THg among the carp species based on their feeding behaviors, with [THg] following the order: herbivore < planktivore < omnivore. However, in a smaller data set ($n = 12$) where trophic position information was available, no differences in [THg], [MMHg], $\delta^{13}C$, or $\delta^{15}N$ were found between the feeding groups. Compared to the BAF of seston (2.7×10^7, average of the two size fractions), BAF increased by a factor of 3, 14, 38, 40, and 54 for the chironomid larvae, herbivore, planktivore, omnivore, and carnivore, respectively. This progressively increasing trend of BAF along the food chain suggests the importance of diet on the bioaccumulation of MMHg for the BR biota.

3.4.3. Reduced uptake of MMHg due to biodilution at the base of food chain

Another factor contributing to the observed low MMHg accumulation in the fish of BR is closely related to the high primary production and biomass in this eutrophic system. At the base of the food chain, high density of algae such as those seen in algal blooms of eutrophic systems would lower the concentration of MMHg per cell, a phenomenon often referred to as “bloom dilution” (Pickhardt et al., 2002). Under high nutrient condition, phytoplankton can also have higher growth rate than its MMHg uptake rate which would lead to reduced MMHg concentration as the cell divide, a phenomenon termed “growth dilution” (Sunda and Huntsman, 1998). Consequently, both dilution effects (hereafter, biodilution) can propagate directly up the food chain to yield high biomass and low MMHg in heterotrophs whose MMHg exposure is mainly through diet. Indeed, experiments under controlled environment have shown that greater algal biomass reduces MMHg concentrations in zooplankton (Karimi et al., 2007; Pickhardt et al., 2002) and in benthic periphyton (Hill and Larsen, 2005). In the natural environment, Chen and Folt (2005) found THg concentrations in phytoplankton and small zooplanktons to be negatively correlated with phytoplankton density in lakes with different physiochemical and biological characteristics. Based on these findings and the eutrophic conditions of BR, we infer that biodilution may also occur in the base of BR food web resulting in low phytoplankton MMHg concentration and contribute to the limited bioaccumulation of MMHg in the fish of BR, whose trophic positions were only approximately two levels higher than phytoplankton.

4. Conclusion

We studied the distribution of THg and MMHg in biotic and abiotic matrices of Baihua Reservoir. Our data showed that the levels of THg and MMHg were elevated in the sediment and in the anoxic layer of the water column due to direct contaminations from industrial activities, as well as in situ methylation in both sediment–water interface and possibly the bottom water. However, BR fish MMHg levels were low and do not appear to pose a health risk.

By further examining the physiochemical profiles of THg and MMHg in abiotic matrices, and MMHg transfer trends in the biota, we suggest three main explanations of the low fish Hg accumulation observed: i) disconnection of high MMHg zone (i.e. anoxic bottom water and sediment–water interface) from the aquatic food web where fish, chironomid, seston were found (i.e. oxic layer); ii) limited MMHg transfer in a relatively simple food web with short food chains; iii) reduced MMHg uptake in phytoplankton at the base of the food chain due to biodilution in this eutrophic reservoir.

Our results show that the bioaccumulation of MMHg in biota depends on not only the MMHg levels in the water but also the bioaccumulation mechanisms along the food chain. Our study also suggests that attempt to reduce eutrophication and anoxia/hypoxia water in systems like BR may inadvertently enhance MMHg transfer in food webs by attenuating the biodilution effect and increasing fish’s accessibility to high MMHg zones. However, biological and physiochemical changes accompanied by eutrophication management can also in turn alter the existing distribution of Hg speciation as well as the net methylation scheme in BR. Further research is needed in order to provide scientific basis for site-specific water quality management.

Acknowledgments

This study is funded by the Sino-Swiss Science and Technology Cooperation (SSSTC, project No. IZL CY2 123975) and the Chinese Academy of Sciences (GJHZ903). We thank Mingyan Gu, Lushen Pan, Qin Cai, Yong Liu, and Lucie Huguet for their assistance in the field sampling; Dr. Sarah Rothenberg, Dr. Jean-Luc Loizeau and Philippe Arpagaus for their assistance in the laboratory analysis; and Dr. Bo-Ping Han for chironomidae identification.

References

Becker, D.S., Bigham, G.N., 1995. Distribution of mercury in the aqautic food-web of Onondaga Lake. New York Water Air and Soil Pollution 80, 563–571.

Benoit, J.M., Gilmour, C.C., Heyes, A., Mason, R.P., Miller, C.L., 2003. Geochemical and biological controls over methylmercury production and degradation in aquatic ecosystems. Biogeochemistry of Environmentally Important Trace Elements 835, 262–297.

Bloom, N., 1989. Determination of picogram levels of methylmercury by aqueous phase ethylation, followed by cryogenic gas-chromatography with cold vapor atomic fluorescence detection. Canadian Journal of Fisheries and Aquatic Sciences 46, 1131–1140.

Bravo, A.G., 2011. Mercury Methylation and Trophic Transfer in Contaminated Freshwater Systems.

Chen, C.Y., Folt, C.L., 2005. High plankton densities reduce mercury biomagnification. Environmental Science & Technology 39, 115–121.

Clarkson, T.W., Magos, L., 2006. The toxicology of mercury and its chemical compounds. Critical Reviews in Toxicology 36, 609–662.

Compeau, G.C., Bartha, R., 1985. Sulfate-reducing bacteria: principal methylators of mercury in anoxic estuarine sediment. Applied and Environmental Microbiology 50, 498–502.

Cossa, D., Coquery, M., Nakhle, K., Claisse, D., 2002. Total mercury and monomethylmercury analysis in marine organisms and sediments. Analysis Methods in Marine Environment.

Feng, X.B., Yan, H.Y., Wang, S.F., Qiu, G.L., Tang, S.L., Shang, L.H., Dai, Q.J., Hou, Y.M., 2004. Seasonal variation of gaseous mercury exchange rate between air and water surface over Baihua reservoir, Guizhou, China. Atmospheric Environment 38, 4721–4732.

Fitzgerald, W.F., Lamborg, C.H., Hammerschmidt, C.R., 2007. Marine biogeochemical cycling of mercury. Chemical Reviews 107, 641–662.

Gobas, F.A.P.C., de Wolf, W., Burkhard, L.P., Verbruggen, E., Plotzke, K., 2009. Revisiting bioaccumulation criteria for POPs and PBT Assessments. Integrated Environmental Assessment and Management 5, 624–637.

Hall, B.D., Bodaly, R.A., Fudge, R.J.P., Rudd, J.W.M., Rosenberg, D.M., 1997. Food as the dominant pathway of methylmercury uptake by fish. Water Air and Soil Pollution 100, 13–24.

He, T., Feng, X., Guo, Y., Qiu, G., Li, Z., Liang, L., Lu, J., 2008. The impact of eutrophication on the biogeochemical cycling of mercury species in a reservoir: a case study from Hongfeng Reservoir, Guizhou, China. Environmental Pollution 154, 56–67.

Hill, W.R., Larsen, I.L., 2005. Growth dilution of metals in microalgal biofilms. Environmental Science & Technology 39, 1513–1518.

Horvat, M., Nolde, N., Fajon, V., Jereb, V., Logar, M., Lojen, S., Jacimovic, R., Falnoga, I., Qu, L.Y., Faganeli, J., Drobne, D., 2003. Total mercury, methylmercury and selenium in mercury polluted areas in the province Guizhou, China. Science of the Total Environment 304, 231–256.

Karimi, R., Chen, C.Y., Pickhardt, P.C., Fisher, N.S., Folt, C.L., 2007. Stoichiometric controls of mercury dilution by growth. Proceedings of the National Academy of Sciences of the United States of America 104, 7477–7482.

Larssen, T., 2010. Mercury in Chinese reservoirs. Environmental Pollution 158, 24–25.

Lawrence, A.L., Mason, R.P., 2001. Factors controlling the bioaccumulation of mercury and methylmercury by the estuarine amphipod *Leptocheirus plumulosus*. Environmental Pollution 111, 217–231.

Li, Q., Han, B., 2007. Dynamics and structure of phytoplankton community in spring in a southern subtropical pumped-water reservoir. Journal of Tropical and Subtropical Botany 15, 294–300.

Li, W., Wu, F., Liu, C., Fu, P., Wang, J., Mei, Y., Wang, L., Guo, J., 2008. Temporal and spatial distributions of dissolved organic carbon and nitrogen in two small lakes on the Southwestern China Plateau. Limnology 9, 163–171.

Marsalek, P., Svobodova, Z., Randak, T., 2007. The content of total mercury and methylmercury in common carp from selected Czech ponds. Aquaculture International 15, 299–304.

Mason, R.P., Reinfelder, J.R., Morel, F.M.M., 1996. Uptake, toxicity, and trophic transfer of mercury in a coastal diatom. Environmental Science & Technology 30, 1835–1845.

McClain, W.C., Chumchal, M.M., Drenner, R.W., Newland, L.W., 2006. Mercury concentrations in fish from Lake Meredith, Texas: implications for the issuance of fish consumption advisories. Environmental Monitoring and Assessment 123, 249–258.

Merritt, K.A., Amirbahman, A., 2009. Mercury methylation dynamics in estuarine and coastal marine environments – A critical review. Earth-Science Reviews 96, 54–66.

Munthe, J., Bodaly, R.A., Branfireun, B.A., Driscoll, C.T., Gilmour, C.C., Harris, R., Horvat, M., Lucotte, M., Malm, O., 2007. Recovery of mercury-contaminated fisheries. Ambio 36, 33–44.

Navarro, A., Quiros, L., Casado, M., Faria, M., Carrasco, L., Benejam, L., Benito, J., Diez, S., Raldua, D., Barata, C., Bayona, J.M., Pina, B., 2009. Physiological responses to mercury in feral carp populations inhabiting the low Ebro River (NE Spain), a historically contaminated site. Aquatic Toxicology 93, 150–157.

Pickhardt, P.C., Folt, C.L., Chen, C.Y., Klaue, B., Blum, J.D., 2002. Algal blooms reduce the uptake of toxic methylmercury in freshwater food webs. Proceedings of the National Academy of Sciences of the United States of America 99, 4419–4423.

Rogowski, D.L., Soucek, D.J., Levengood, J.M., Johnson, S.R., Chick, J.H., Dettmers, J.M., Pegg, M.A., Epifanio, J.M., 2009. Contaminant concentrations in Asian carps, invasive species in the Mississippi and Illinois Rivers. Environmental Monitoring and Assessment 157, 211–222.

Suchanek, T.H., 2008. Mercury cycling and bioaccumulation in a mine-dominated aquatic ecosystem: clear lake, California. Ecological Applications 18, A1–A2.

Sunda, W.G., Huntsman, S.A., 1998. Processes regulating cellular metal accumulation and physiological effects: phytoplankton as model systems. Science of the Total Environment 219, 165–181.

Todorova, S.G., Driscoll, C.T., Matthews, D.A., Effler, S.W., Hines, M.E., Henry, E.A., 2009. Evidence for Regulation of monomethyl mercury by nitrate in a seasonally stratified, eutrophic Lake. Environmental Science & Technology 43, 6572–6578.

Ullrich, S.M., Tanton, T.W., Abdrashitova, S.A., 2001. Mercury in the aquatic environment: a review of factors affecting methylation. Critical Reviews in Environmental Science and Technology 31, 241–293.

USEPA, 2010. User's Guide and Technical Documentation KABAM Version 1.0 (Kow (Based) Aquatic BioAccumulation Model). http://www.epa.gov/oppefed1/models/water/kabam/kabam_user_guide_appendix_c.html Appendix C,.

Wang, S., Zhu, J., Ma, M., Yin, C., Liu, C., 2005. Thermal stratification and paroxysmal deterioration of water quality in a canyon-reservoir, southwestern China. Journal of Lake Sciences 17, 54–60.

Watras, C.J., Back, R.C., Halvorsen, S., Hudson, R.J.M., Morrison, K.A., Wente, S.P., 1998. Bioaccumulation of mercury in pelagic freshwater food webs. Science of the Total Environment 219, 183–208.

Yan, H., 2005. The methodological development of mercury species in environmental samples and the primary study on biogeochemical cycling character of mercury in Baihua Reservoir in Guizhou. Ph. D. dissertation, Chinese Academy of Sciences.

Yan, H., Feng, X., Tang, S., Shang, L., Wang, S., Dai, Q., Hou, Y., 2003. The concentration and distribution of different mercury species in the water columns of BaiHua reservoir. Journal De Physique Iv 107, 1385–1388.

Yan, H.Y., Feng, X.B., Shang, L.H., Qiu, G.L., Dai, Q.J., Wang, S.F., Hou, Y.M., 2008. The variations of mercury in sediment profiles from a historically mercury-contaminated reservoir, Guizhou province, China. Science of the Total Environment 407, 497–506.

Yan, H.Y., Rustadbakken, A., Yao, H., Larssen, T., Feng, X.B., Liu, T., Shang, L.H., Haugen, T.O., 2010. Total mercury in wild fish in Guizhou reservoirs, China. Journal of Environmental Sciences-China 22, 1129–1136.

Zhang, W., 2000. Pollutions and management strategies of Baihua Reservoir Guizhou. Environmental Sciences and Technology 6, 23–28.

Zhou, H.Y., Wong, M.H., 2000. Mercury accumulation in freshwater fish with emphasis on the dietary influence. Water Resources 34, 4234–4242.